

High temperature corrosion of low alloyed steel in air and salt mist atmospheres

Korozja wysokotemperaturowa niskostopowych stali wygrzewanych w powietrzu i atmosferze mgły solnej

Tomasz Dudziak¹, Konrad Jura²

¹ Instytut Odlewnictwa, Centrum Badań Wysokotemperaturowych, ul. Zakopiańska 73, 30-418 Kraków

² EDF Polska, R&D Centre, ul. Ciepłownicza 1, 31-587 Kraków

¹ Foundry Research Institute, Centre for High Temperature Studies, ul. Zakopiańska 73, 30-418 Kraków, Poland

² EDF Polska, R&D Centre, ul. Ciepłownicza 1, 31-587 Kraków, Poland

E-mail: tomasz.dudziak@iod.krakow.pl

Received: 7.04.2016. Accepted in revised form: 30.06.2016.

© 2016 Instytut Odlewnictwa. All rights reserved.

DOI: 10.7356/iod.2016.07

Abstract

The aim of this work has been to show the influence of air oxidation and salt mist corrosion on the behaviour of low alloyed steels 18K (K18), 16M (16Mo3), 15HM (13CrMo4-4) and finally 10CrMo9-10 (10H2M) employed in the Polish energy sector. The exposures have been carried out at 450°C, 500°C, and finally 550°C for 500 hours. The obtained results indicate that in both atmospheres, the exposed steels developed similar phases containing Fe₃O₄ (magnetite) and Fe₂O₃ (hematite). The scale thicknesses developed under both corrosion conditions have indicated similar values. On the other hand, the addition of 1% NaCl – 1% Na₂SO₄ to deionised water generates the development of layered structures on low-alloyed steels with different Fe₂O₃ and Fe₃O₄ ratio, the effect originates most probably from the presence of S and Cl within the oxide scale. The presence of layers with different phase ratio generates the formation of stresses originating from different coefficients of thermal expansion (CTE) between the phases (Fe₂O₃, Fe₃O₄) and between the layers themselves.

Keywords: air oxidation, salt mist corrosion, high temperature

Streszczenie

W artykule opisano zagadnienia związane z korozją wysokotemperaturową stali niskostopowych 18K (K18), 16M (16Mo3), 15HM (13CrMo4-4) oraz 10CrMo9-10 (10H2M), które są często stosowane w polskim sektorze energetycznym. Testy wysokotemperaturowe zostały wykonane

w temperaturach 450°C, 500°C i 550°C przez okres 500 godzin. Otrzymane wyniki pokazują, iż w dwóch różnych atmosferach korozyjnych, stale niskostopowe wytworzyły takie same fazy, głównie Fe₂O₃ (hematyt) oraz Fe₃O₄ (magnetyt) z tą różnicą, iż w atmosferze mgły solnej zawierającej 1% NaCl – 1% Na₂SO₄ zgorzelina tlenkowa miała charakter warstwowy. Charakter ten prawdopodobnie zawdzięcza jest obecności S i Cl wewnątrz zgorzeliny tlenkowej, co więcej warstwy różnią się zawartością Fe₂O₃ oraz Fe₃O₄, co powoduje powstawanie naprężeń, tendencje do odpadania z powodu różnych wartości współczynnika rozszerzalności cieplnej między fazami Fe₂O₃ oraz Fe₃O₄, a także między warstwami.

Słowa kluczowe: utlenianie w powietrzu, mgła solna, wysoka temperatura

1. Introduction

Scientific research plays an important role in order to understand the existing world and the phenomena behind the micro scale. In modern civilisation, one of the most important issues is energy conversion; production is corrosion degradation of the materials exposed at high temperatures. The materials dedicated for power plant constructions (waterwalls, header, super-heaters, and re-heaters) are facing various high temperature regimes like oxidising, reducing, mixed environments with presence of CO and CO₂. Currently, coal power plants using pulverised fuel are still a main contributor in energy production and environmental pollution due to the high

emission of CO₂ gas. Nevertheless, there is the possibility to decrease CO₂ emission due to higher temperature when coal is burned, and increase pressure in the steam system. New coal fired power plants with higher efficiency and less polluted character require modern materials to withstand high temperature regimes, coating high amounts of Cr in the metal matrix in order to develop highly protective Cr₂O₃ scale [1]. Regrettably, the construction of brand new, clean, eco-friendly high efficiency power plants require costly investments, hence around the world there are still in existence many low efficiency, highly polluted coal fired power plants in operation. The European Union (EU) has put restricted legislation in place in order to significantly reduce emissions from EU coal fired power stations to 20% by the year 2020 in reference to the level in 1990 [2]. Generally speaking, a 1% increase in absolute efficiency in a power plant results in as much as a 3% reduction in CO₂ emissions [3]. In recent years, the observed significant changes in electric power sector related to reducing CO₂ emissions are strictly associated to ground breaking developments in material science and engineering. Throughout the last decades, tremendous progress has been achieved in the development of steels and technologies associated with energy production. Progress in steels performance for coal fired power can be illustrated by the following numbers of outlet steam pressure and temperatures [4]:

1. 70s of XX century: T = 538°C / 538°C / 16.7 MPa (167 bar).
2. 80s of XX century: T = 540°C / 560°C / 25.0 MPa (250 bar).
3. 90s of XX century: T = 560°C / 580°C / 27.0 MPa (270 bar).
4. Turn of the century XX–XXI: T = 600°C / 620°C / 29,0 MPa (290 bar) USC.
5. In 2020 of XXI century: T = 700°C / 720°C / 350 MPa (350 bar) AUSC.

Together with increasing temperatures in coal fired power plant, performance of the materials designed for the energy sector, as well show expansion [5]:

1. Ferritic steels: p < 26 MPa (260 bar), T = 545°C.
2. Ferritic martensitic steels: p = 26 MPa (260 bar), T = 545°C.
3. Austenitic steels: p = 29 MPa (290 bar), T = 600°C.
4. Ni based alloys: p > 35 MPa (350 bar), T > 700°C.

Development of Ultrasuper Critical (USC) and Advanced Ultrasuper Critical (AUSC) coal fired power plants requires high performance steels and Ni based superalloys, therefore constant research programme and projects obeying development of new materials need to be carried out in the laboratory scale test rigs. Since low-alloyed steels show limited performance at high temperatures and cannot be used in temperature ranges higher than 600°C due to the formation of non-protective scales. The study presents the results of air oxidation and salt mist corrosion experiments to indicate significance of corrosion issues in terms of materials performance. In this work, only low-alloyed steels and relatively high temperature conditions have been selected, the materials have been exposed in a temperature range 450–550°C for 500 hours. The materials have been investigated using standard procedure including Scanning Electron Microscope (SEM) coupled with Energy Dispersive X-Ray Spectrometry.

2. Experimental procedure

The general procedure of the sample preparation to high temperature tests is shown below. In this work, the selected results are shown including air oxidation, salt mist corrosion and steam oxidation. In air and salt mist corrosion, low alloyed steels have been tested, whereas in steam oxidation atmosphere only highly alloyed materials including Fe based materials have been studied. The tested parameters and the materials selection for high temperature testing were based on materials limitation; low alloyed steels due to the formation of less protective scales have been tested at lower temperatures. Prior to high temperature investigations the samples with dimensions around 1 cm × 1 cm, and the thickness around 0.4 cm, were cut off using a precise cutting saw. Following the cutting process, the samples were firstly grounded using different SiC papers and polished with diamond suspension pastes. The polished steel samples have been accurately measured using a micrometer. A further step in sample preparation prior to the high temperature tests has involved ultrasonic cleaning for 15 min at 40°C. Finally, the steel samples were weighted to obtain initial masses of the individual material.

2.1 Materials

In the study, low alloyed steels 18K (K18), 16M (16Mo3), 15HM (13CrMo4-4) and finally 10CrMo9-10 (10H2M) have been used, chemical composition is shown in Table 1 based on certificates delivered from the funding body.

Table 1. Chemical composition of low alloyed steels used in air and salt mist corrosion, wt. %
 Tabela 1. Skład chemiczny stopów na bazie żelaza użytych w badaniach w powietrzu i mgle solnej, % wag.

Grade/Gatunek		Chemical composition, wt. % / Skład chemiczny stopów, % wag.									
		C	Mn	Si	P max.	S max.	Cr max.	Ni max.	Cu max.	Mo	Other
K18	18K	0.16–0.22	min. 0.60	0.10–0.35	0.045	0.045	0.20	0.35	0.25	–	–
16Mo3	16M	0.12–0.20	0.50–0.80	0.15–0.35	0.040	0.040	0.30	0.35	0.25	0.25–0.35	Al max. 0.02
13CrMo4-4	15HM	0.11–0.18	0.40–0.70	0.15–0.35	0.040	0.040	0.70–1.00	0.35	0.25	0.40–0.55	Al max. 0.02
10CrMo9-10	10H2M	0.08–0.15	0.40–0.60	0.15–0.50	0.003	0.030	2.00–2.50	0.30	0.25	0.90–1.10	Al max. 0.02

2.2 Air oxidation

The high temperature tests in atmospheric air have been conducted in the rig presented schematically in Figure 1.

The rig presented in Figure 1 has been used in order to carry out the tests in atmospheric air at high temperatures. The test rig accommodated the samples in the hot zone of the furnace; the hot zone of the furnace prior to the test has been accurately calibrated using thermocouple K and digital thermometer. The furnace has been calibrated for tests at 450°C, 500°C and 550°C. Each of the tests have been designed for 500 hours, while every 100 h the furnace has been automatically turned

off and has cooled down to achieved room temperature. Furthermore, the exposed low-alloyed steel samples in the furnace have been withdrawn and accurately weighed to obtain kinetic data determining corrosion performance at high temperatures. During the high temperature tests in air, ceramic isolators have sealed the ends of the ceramic liner tube in order to avoid thermal shocks invoked by humid air from the outside.

2.3 Salt spray corrosion

Schematic illustration in Figure 2 presents salt spray corrosion experimental rig.

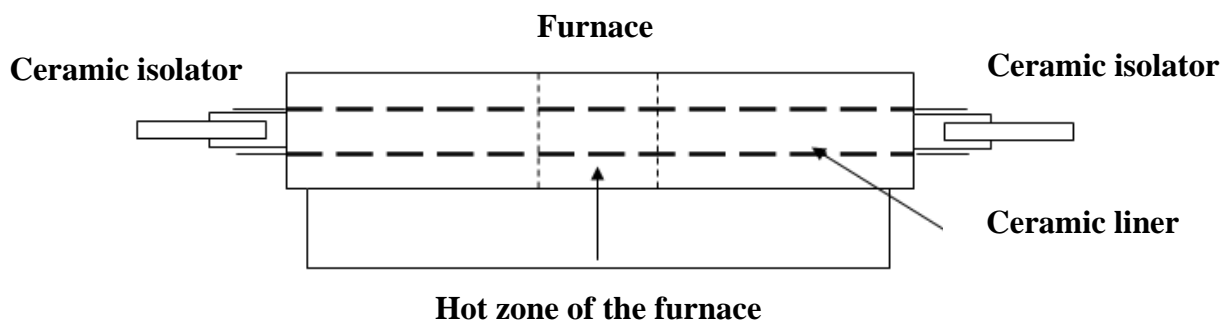


Fig. 1. High temperature rig for air oxidation experiments used in this project

Rys. 1. Układ do badań wysokotemperaturowych w powietrzu

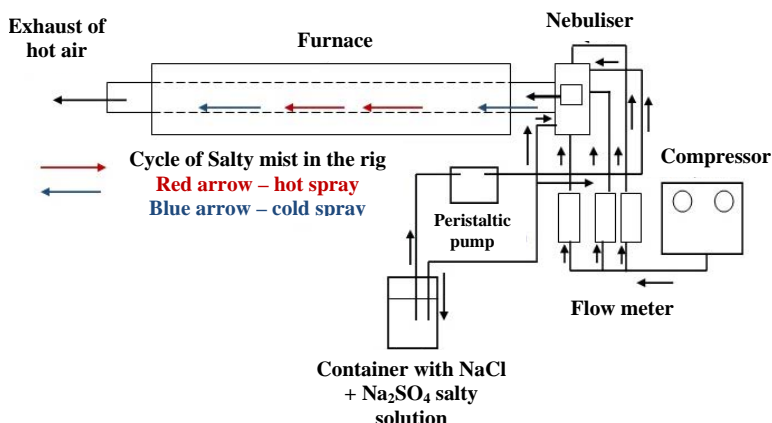


Fig. 2. Schematic illustration of salt spray test rig containing 1% NaCl – 1% Na₂SO₄ salt solution

Rys. 2. Schemat ilustrujący układ do badań w atmosferze mgły solnej zawierającej roztwór 1% NaCl – 1% Na₂SO₄

The low-alloyed steel samples listed in Table 1 were placed in an experimental test rig and were exposed to salt spray at 450°C, 500°C and 550°C. The salt mist conditions were created from the salt solution containing 1% NaCl and 1% Na₂SO₄. Low concentrated salt spray mixture was used in this test in order to avoid clogging of the nozzle; the nozzle undergoes clogging while more concentrated mixture of salt is used due to the tiny dimension of the nozzle hole. The samples after the preparation procedure described in detail previously were placed in the hot zone of the furnace. When the furnace reached 200°C, the compressor was turned on in order to pump the salt solution from the container below the furnace. The salt solution was pumped from the container by a peristaltic pump to the nebuliser where tubing with compressed air was connected in order to create the spray under pressure. The pressure of the mist entering the furnace was controlled by flow meter controllers. When the cold salt spray entered the nozzle under pressure and reached the hot zone of the furnace (where the samples were placed), transformation into water steam with salt solution containing 1% NaCl – 1% Na₂SO₄ occurred. The salt spray under pressure washed around the samples placed in the furnace, while later the mist has been exhausted from the furnace by the hole in the back flanche attached in the ceramic liner.

3. Results and discussion

This section describes the results of high temperature exposures of low alloyed steels in air and salt spray corrosion atmosphere for 500 hours at 450°C, 500°C and 550°C.

3.1 Air oxidation

Figures 3A–C shows the kinetic results of high temperature air oxidation of the boiler steels in temperature range 450–550°C.

As shown in Figures 3A–C, the highest mass gain has been observed for the samples exposed at 550°C, whereas the lowest mass gain has been observed at 450°C. Furthermore, the sample with the highest concentration of Cr (10H2M steel) formed the oxide scale with poor adhesion to the substrate (Fig. 3). The sample 10H2M showed as well unstable behaviour at 500°C and 550°C. The other steels (18K, 16M and 15HM) showed more steady state oxidation behaviour with no scale delamination spallation observed within 500 h. The steels formed more adherent scale than that observed in 10H2M material. Cross sections of the exposed materials confirm the findings from kinetic results. Figure 4 reveals that all the exposed materials developed relatively thick oxide scale at 450–550°C.

The formation of the oxide scales on the boiler steels 18K, 16M, 15HM and 10H2M with different concentra-

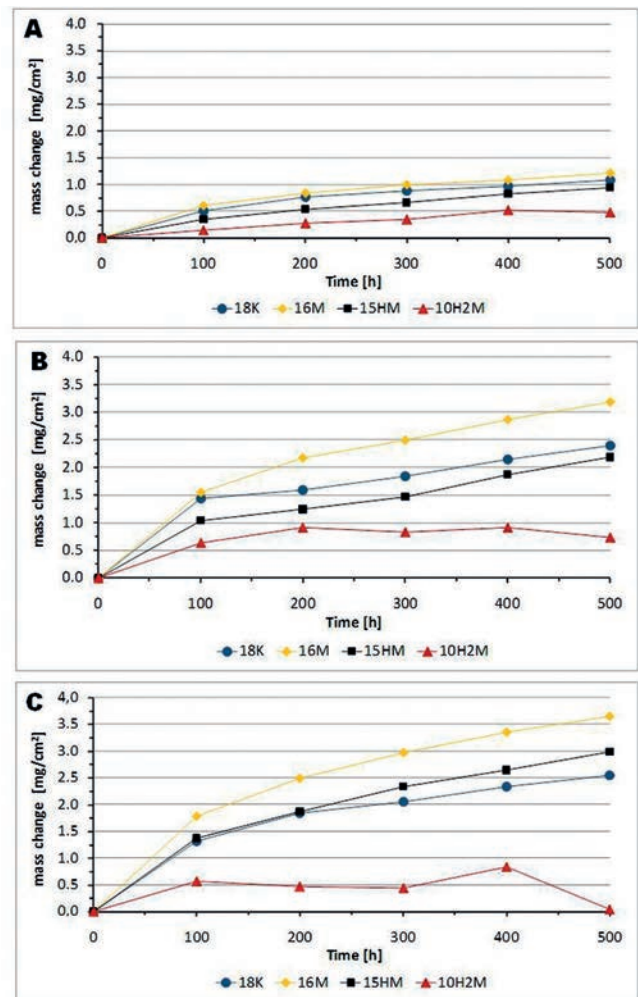


Fig. 3. Mass change for the materials exposed for 500 hours at high temperatures A) 450°C, B) 500°C and C) 550°C in air

Rys. 3. Zmiana masy dla materiałów na bazie żelaza wygrzewanych przez okres 500 h w temperaturze A) 450°C, B) 500°C and C) 550°C w powietrzu

tion of Cr showed limited oxidation resistance at high temperatures. The oxide scales developed at high temperatures showed poor adhesion to the metallic substrate, a number of cracks have been observed as well perpendicular to the metal surface, suggesting that the formed oxide scales are brittle and may easily exfoliate from the metallic substrate under thermal cycling, when the temperature is unstable. High concern has been found while 18K boiler steel showed the cracked formed through the grain boundaries under high temperature regime. The observed crack can seriously accelerate degradation of the material especially in the harsh environment where different conditions are met. Moreover it has been found, that the number of steels have been contaminated by sulphur phases (EDX confirmed), the impurity zones are indicated by the white circles on SEM pictures presented in Figure 4. The low-alloyed steels

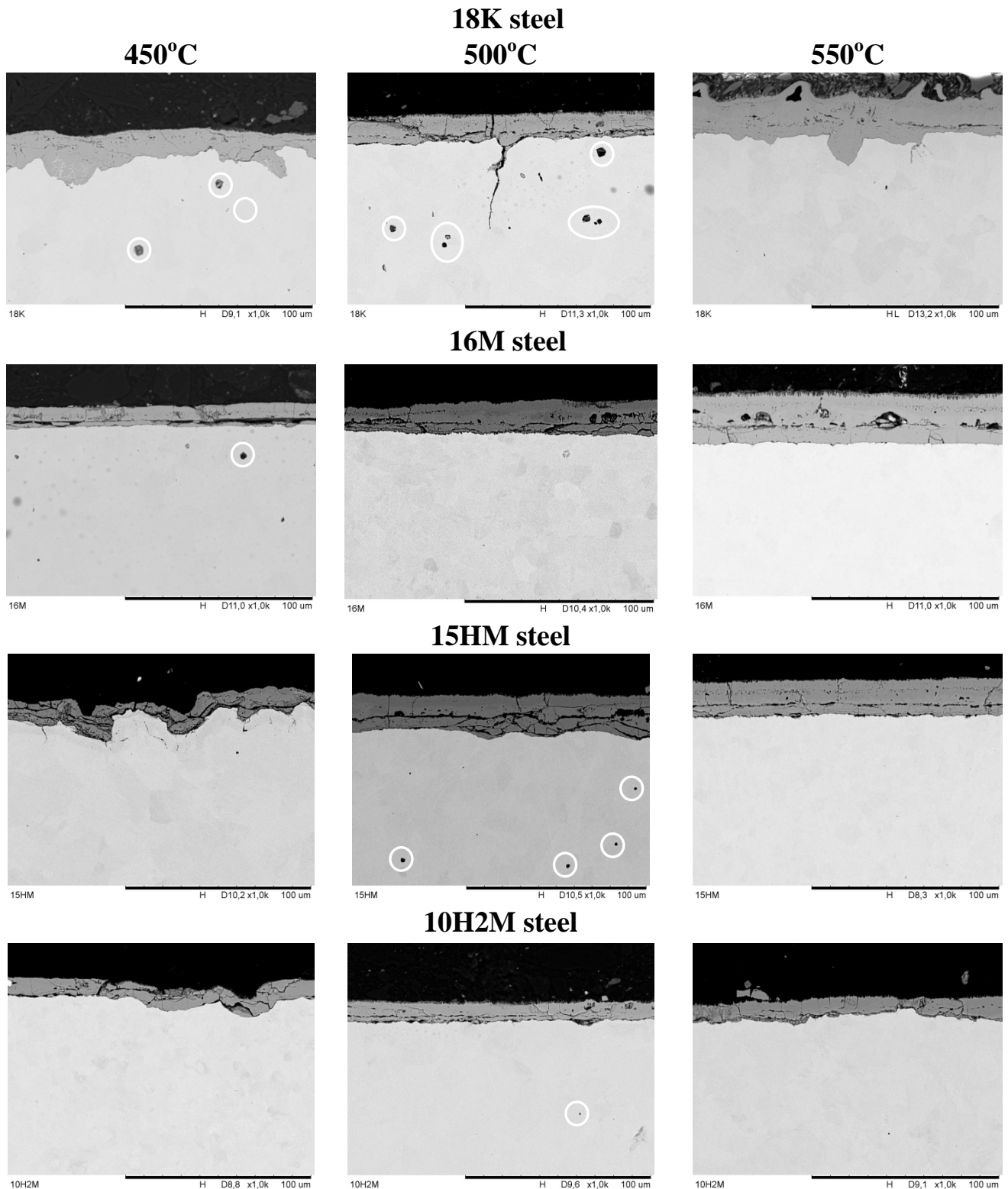
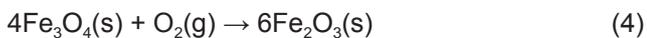
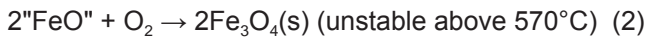


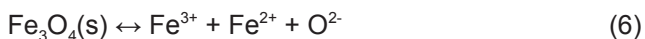
Fig. 4. Cross-sectioned images performed by means of SEM in BSE mode after 500 h exposures at 450°C (left), 500°C (middle) and 550°C (right) for 18K, 16M, 15HM and 10H2M steels in atmospheric air

Rys. 4. Zdjęcia z przekrojów poprzecznych wykonanych w technice BSE po wygrzewaniu w temperaturze 450°C (zdjęcie lewe), 500°C (środkowe) oraz 550°C (prawe) stali 18K, 16M, 15HM oraz 10H2M w powietrzu

examined under an EDX analyser showed very similar chemical representations. In general the top layer of the oxide scale has been invaded by hematite (Fe_2O_3), the innermost layer has been occupied by magnetite (Fe_3O_4), and the steels with Cr content in the range of 1–2.5 wt. % (15HM, 10H2M) showed the formation of tiny islands rich in Cr between the substrate and the oxide scale. The observations and findings are well confirmed by previous experiments conducted by Wright et al. [6], Lépingle et al. [7] and other researchers [8, 9, 10]. The formation of oxide layers is governed mainly by Gibbs free energy formation and partial pressure of oxygen in the ambient atmosphere. Since FeO is unstable at 550°C and other temperatures in this study, therefore the oxide scale consisted of two main compounds, Fe_3O_4 (magnetite) and Fe_2O_3 (hematite), the formation of Fe_3O_4 is slightly more stable than Fe_2O_3 due to more negative Gibbs free energy formation, up to 570°C. Furthermore, at this temperature Fe_3O_4 undergoes a dissociation process.



Dissociation of Fe_3O_4 phase at the interface with the inner and outer layer of the released iron ions may diffuse to the oxide-gas interface to react and form new oxide [11]. According to Fujii et al. [12, 13], the inner layer (Fe_3O_4) dissociates according to the reaction shown below:



The dissociation of magnetite released iron ions, which feed and accelerate development of FeO which is more stable at higher temperatures than Fe_3O_4 (magnetite). Nevertheless, in this work, formation of FeO is omitted, since experiments have been conducted up to 570°C.

3.2 Salt spray corrosion

Figures 5A–C shows the kinetic results of the low alloyed steels exposed for salt spray atmospheric corrosion using 1% NaCl – 1% Na_2SO_4 solution for 500 hours at 450–550°C.

In contrast to the results presented in Figure 4 oxidation kinetics in the solution of 1% NaCl – 1% Na_2SO_4 showed different influences on the exposed steels. At 450°C for 500 h only 15HM alloy presented accept-

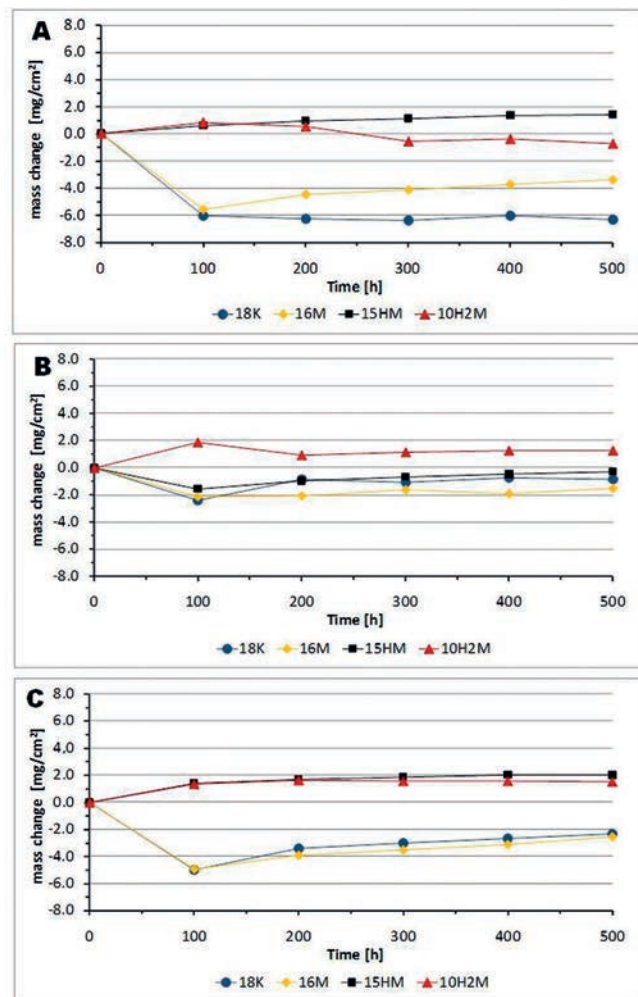


Fig. 5. Mass change for the materials exposed for 500 hours at high temperatures A) 450°C, B) 500°C and C) 550°C in salt spray corrosion

Rys. 5. Zmiana masy dla materiałów na bazie żelaza wygrzewanych przez okres 500 h w temperaturze A) 450°C, B) 500°C and C) 550°C w atmosferze mgły solnej

able behaviour where lack of scale delamination has been observed. The 10H2M alloy with the highest Cr content in the bulk steel after 200 hours of the exposure showed lowering in mass change, this decrease can be explained by the scale of delamination spallation. Two other materials 18K and 16M showed lack of protectiveness in the beginning of the high temperature tests, where spallation occurred, however later the alloys showed steady oxidation kinetics where no spallation has been observed at 450°C. Under slightly higher temperature (500°C), the 10H2M steel showed mass increases upon high temperature exposure, however after 100 h, its mass decreased to $m = 1 \text{ mg/cm}^2$ showing the constant mass up to end of the test (500 hours). Such behaviour of the 10H2M alloy indicates high thermodynamic stability of the system upon salt spray at 500°C. The exposure in the highest tempera-

ture revealed that the addition of a tiny amount of Cr to the bulk steel shows some positive effect. Two low alloyed steels 18K and 16M showed poorer behaviour under test conditions where mass dropped in the beginning of the test and reached -3 mg/cm^2 . However, the alloys with 1 and 2.5 wt. % addition of Cr (15HM, 10H2M respectively) indicate a positive effect where low mass gain has been observed with lack of delamination spallation of the external oxide scale.

3.2.1 Cross section investigations

Similarly, to the air oxidation experiment, the samples exposed to salt spray corrosion atmosphere have been cross-sectioned in order to evaluate corrosion degradation, oxide thickness developed at high temperatures. The results are shown in [Figure 6](#).

Similar to air oxidation exposures, the low alloyed steel exposed in an atmospheric salt spray environment developed mainly Fe_3O_4 and Fe_2O_3 within the scale at high temperatures $450\text{--}550^\circ\text{C}$. The scale developed upon salt spray mixture solution with 1% NaCl – 1% Na_2SO_4 showed formation of oxide scale where the top layer was mostly occupied by hematite (Fe_2O_3) with some spots of magnetite (Fe_3O_4). Due to the high degree of porosity observed throughout the SEM investigations, the oxide scale underwent the formation of elongated cracks. The inner part of the oxide scale contained large amounts of Fe_3O_4 . Further, EDX analyses performed on the cross-sectioned samples showed that sulphur and other salty compounds were delivered to the oxide scale through the decomposition of the salts under high temperature. The low concentrated salty compounds in the oxide scale originate due to the low concentrated salt solution used in this work. Due to low concentration of the salt mixture in salt spray corrosion tests at high temperatures, the enrichment of S or Cl on the exposed surfaces has not been detected via EDX analyses, however presence of S and Cl has been found, furthermore, it has been found under EDX analyses, that within the oxide scale areas with S and Cl presence have been observed. The behavior suggests that despite low concentrated salt spray, activity of both S and Cl was high enough to diffuse inside the oxide scale throughout the defects. It is well known, that phases based on Fe-S and Fe-Cl structures are subjected to high defect ratio [14, 15] and secondly Fe-Cl phases are extremely unstable [16]. Such behavior may greatly influence the formation of the layered structures observed under salt spray corrosion, where local formation of defected Fe-S like phases and Fe-Cl like phases have developed. Moreover, it has been found, that the addition of a small portion of salt mixture to the deionized water invokes the formation of the oxide scale with completely different morphology, than that observed in air oxidized low alloyed steels. The salt spray corrosion experiment revealed, that the presence of tiny amounts of salt invokes

the oxide scale developed at high temperatures which showed much poorer adhesion, more cracks and more layered structures formed in every part of the exposed material. The findings confirm kinetic results, where spallation occurred, the spallation and exfoliation of the oxide scale occurs when coefficient of thermal expansion (CTE) between two different layers or phases. In this case, cross-sectioned images shown, the materials indicate layered structures, where mainly Fe_3O_4 and Fe_2O_3 have been found, however the layers consisting of different ratio of Fe_2O_3 to Fe_3O_4 and vice versa, as shown via [reactions 1–6](#). Hence the structures formed under salt spray corrosion are similar in terms of phase constituents, nevertheless, the addition of tiny amounts of salt changes oxide scale structures and behavior for more brittle and less protective that under air oxidation conditions unstable in terms of thermal exposure and expansion. It is important to note, that the amount of Cr in the bulk steel showed no influence on general corrosion behavior, the thickness of the oxide scale developed on the 10H2M steel showed similar value as that formed on the steel with the lowest concentration of Cr (18K). Due to the relatively low salt concentration in the mist, the mechanism of oxide scale formation can be adopted from the air oxidation process.

4. Conclusions

The coupons of boiler tubes underwent severe corrosion degradation at high temperatures in the atmosphere of atmospheric air under 1 bar pressure. Due to the similarity in chemical composition of the alloys used in the tests, the materials developed oxide scales containing a mixture of hematite (Fe_2O_3) and magnetite (Fe_3O_4). The innermost layer of the formed oxide scale presents mainly forms in the magnetite phase (Fe_3O_4). The formation of wustite (FeO) was not observed, the wustite phase (FeO) forms at higher temperatures than that carried out in the following research, wustite phase (FeO) is stable at temperatures above 570°C . The formed oxide scales showed porosity and poor adhesion to the metallic substrate; the 18K alloy underwent stress corrosion cracking under a high temperature regime at 500°C with a length of $50 \mu\text{m}$. The coupons under salt spray corrosion atmosphere developed as well thick, non adhesive structures containing traces of chlorine and sulphur; these elements have been found on their surfaces and at the oxide scale/metallic substrate interface. In addition, the oxide scales show the same phase structures however layered structures observed under salt mist corrosion contained a different ration of Fe_2O_3 and Fe_3O_4 , leading to thermal stress development due to the different coefficient of thermal expansion (CET). The 10H2M steel with the highest Cr content (2.5 wt. %) showed development of islands rich in Cr at the oxide scale interface with concentration up to 4 wt. %.

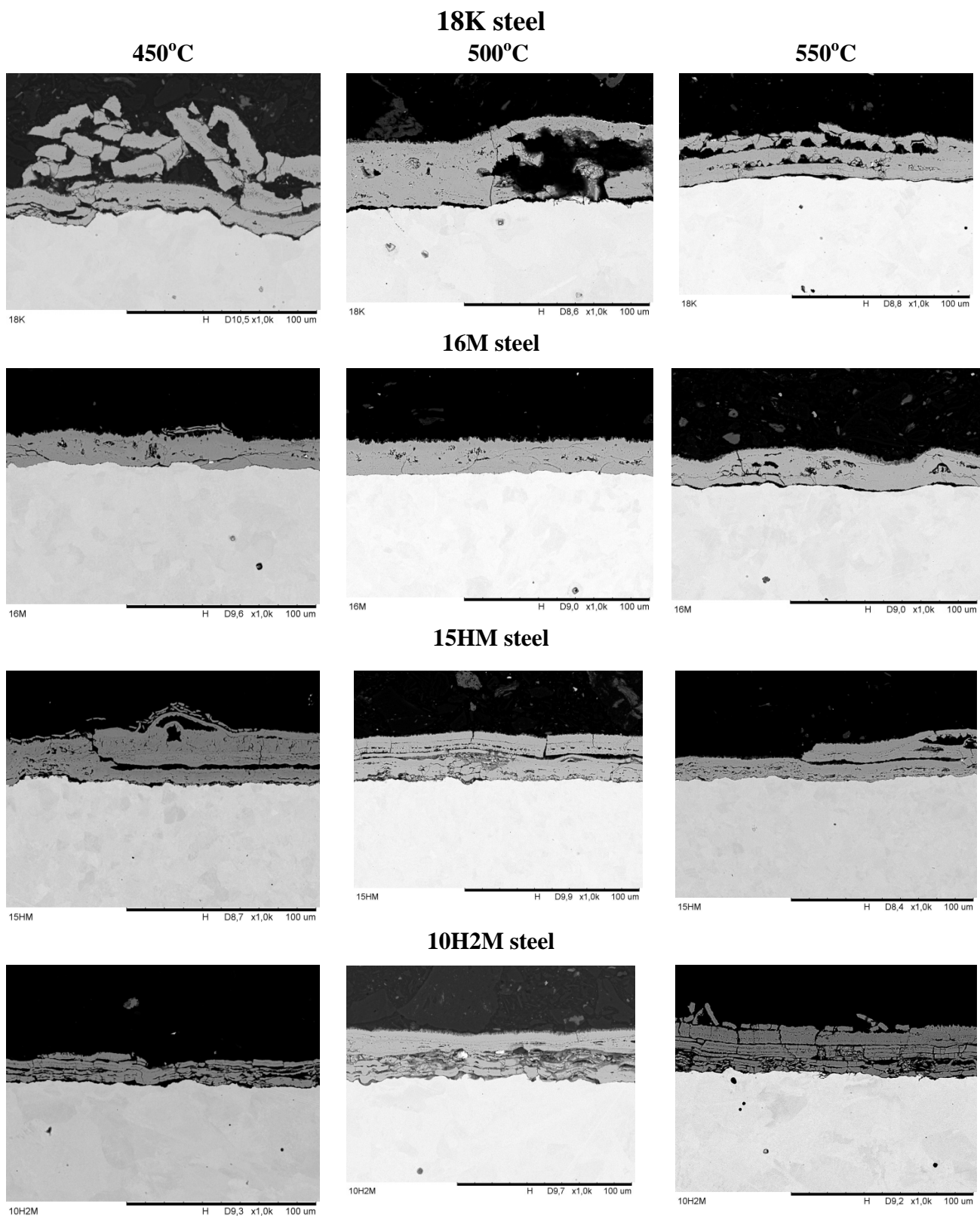


Fig. 6. Cross sectional images of the alloys 18K, 16M, 15HM and 10H2M exposed in salt spray mixture containing 1% NaCl – 1% Na₂SO₄ at 450°C (right), 500°C (middle) and 550°C (right) for 500 h

Rys. 6. Zdjęcia z przekrojów poprzecznych wykonanych w technice BSE po wygrzewaniu w temperaturze 450°C (zdjęcie lewe), 500°C (środkowe) oraz 550°C (prawe) stali 18K, 16M, 15HM oraz 10H2M w atmosferze mgły solnej

Acknowledgment

Authors like to acknowledge the financial support of EDF Polska. The study was a part of the project "Fundamental research of high temperature resistance of boiler steels". Grant number: R&D/ZN/KWA/04072014/099.

References

1. Deodeshmukh V.P. 2013. "Long-Term Performance of High-Temperature Foil Alloys in Water Vapor Containing Environment. Part I: Oxidation Behavior". *Oxidation of Metals* 79 (5–6) : 567–578, DOI 10.1007/s11085-012-9343-1.
2. Traynor I., D. Gow. 2007. "EU promises 20% reduction in carbon emissions by 2020". *The Guardian Newspaper*, Wednesday 21 February 2007.
3. Henry J., G. Zhou, T. Ward. 2007. "Lessons from the past: materials-related issues in an ultra-supercritical boiler at Eddystone plant". *Materials at High Temperatures* 24 (4) : 249–258.
4. Kern T.U., K. Weighthardt, H. Kirchner. 2004. Material and design solutions for advanced steam power plants. In *Proceedings of the Fourth International Conference on Advances in Materials Technology for Fossil Power Plants*. Hilton Head Island, USA.
5. Wright I.G., R.B. Dooley. 2010. "A review of the oxidation behaviour of structural alloys in steam". *International Materials Reviews* 55 (3) : 129–167.
6. Wright I.G., B.A. Pint. 2002. An assessment of the high-temperature oxidation behaviour of Fe-Cr steels in water vapour and steam. USA NACE Corrosion, Denver, CO, 8–11 April 2002, paper no. 02377.
7. Lépingle V., G. Louis, D. Petelot, B. Lefebvre, J. Vaillant. 2001. "High Temperature Corrosion Behaviour of some Boiler Steels in Pure Water Vapour". *Materials Science Forum* 369–372 : 239–246.
8. Sánchez L., M.P. Hierro, F.J. Pérez. 2009. "Effect of chromium content on the oxidation behaviour of ferritic steels for applications in steam atmospheres at high temperatures". *Oxidation of Metals* 71 (3–4) : 173–186.
9. Saunders S.R.J., L.N. McCartney. 2006. "Current Understanding of Steam Oxidation – Power Plant and Laboratory Experience". *Materials Science Forum* 522–523 : 119–128.
10. Fry A., S. Osgerby, M. Wright. 2002. *Oxidation of Alloys in Steam Environments – A Review*. UK: National Physical Laboratory.
11. Stott F., I. Wright, T. Hodgkiess, G. Wood. 1977. "Factors affecting the high-temperature oxidation behavior of some dilute nickel- and cobalt-base alloys". *Oxidation of Metals* 11 (3): 141–150.
12. Fujii C.T., R.A. Meussner. 1964. "The mechanisms of the high-temperature oxidation of iron-chromium alloys in water vapour". *Journal of the Electrochemical Society* 111 (11) : 1215–1221.
13. Fujii C.T., R.A. Meussner. 1963. "Oxide structures produced on iron-chromium alloys by a dissociative mechanism". *Journal of the Electrochemical Society* 110 (12) : 1195–1204.
14. Fasiska E.J. 1972. "Some defect structures of iron sulfide". *Physica Status Solidi A* 10 (1) : 169–173.
15. Jansson S., W. Hübner, G. Östberg, M. de Pourbaix. 1969. "Oxidation resistance of some stainless steels and nickel-based alloys in high-temperature water and steam". *British Corrosion Journal* 4 (1) : 21–31.
16. Dudziak T., K. Jura, J. Rutkowska. 2016. "Chlorine corrosion degradation of low alloyed ferritic steels in temperature range 450–550°C". *Oxidation of Metals* 85 : 647–664, DOI 10.1007/s11085-016-9617-0.

